PROCEEDINGS OF SPIE

SPIEDigitalLibrary.org/conference-proceedings-of-spie

GaAsP nanowires and nanowire devices grown on silicon substrates

Yunyan Zhang
Martin Aagesen
Ana M. Sanchez
Richard Beanland
Jiang Wu
Huiyun Liu

SPIE.

GaAsP Nanowires and Nanowire Devices Grown on Silicon Substrates

Yunyan Zhang[a], Martin Aagesen [b], Ana M. Sanchez[c], Richard Beanland[c], Jiang Wu [a], Huiyun Liu [a,*]

[a] Department of Electronic and Electrical Engineering, University College London, London WC1E 7JE, United Kingdom;
[b] Gasp Solar ApS, Gregersensvej 7, Taastrup DK-2630, Denmark;
[c] Department of Physics, University of Warwick, Coventry CV4 7AL, United Kingdom

ABSTRACT

Ternary GaAsP nanowires (NWs) have gained great attention due to their structure-induced novel properties and band gap that can cover the working wavelength from green to infrared. However, the growth and hence applications of self-catalyzed GaAsP NWs are troubled by the difficulties in controlling P and the complexities in growing ternary NWs. In this work, self-catalyzed core-shell GaAsP NWs were successfully grown and demonstrated almost stacking-fault-free zinc blend crystal structure. By using these core-shell GaAsP NWs, single NW solar cells have been fabricated and a single NW world record efficiency of 10.2% has been achieved. Those NWs also demonstrated their potential application in water splitting. A wafer-scale solar-to-hydrogen conversion efficiency of 0.5% has been achieved despite the low surface coverage. These results open up new perspectives for integrating III−V nanowire photovoltaics on a silicon platform by using self-catalyzed GaAsP core−shell nanowires.

Keywords: self-catalyzed, GaAsP, Nanowire.

1. INTRODUCTION

Nanowires (NWs) with a one-dimensional (1D) columnar shape have better functionality, superior performance, higher integration ability and lower cost.[1-4] Recently, they have gained great attention and been envisioned as a next-generation technology to solve limitations in traditional thin film epitaxial technique. For example, the requirement of lattice and thermal expansion coefficient can be greatly alleviated, giving more freedom in the material combination and the substrate choice. [5-11] III−Vs and Si can thus be monolithically integrated, which is a goal pursued for more than 40 years. In addition, the NW geometry can give new theories for the band structure engineering and hence the device structure design.[12] For example, strain-free quantum dots (QDs) can be grown by stacking the material axially.[13] Therefore, QDs can be fabricated with a wider range of materials as compared with the traditional Stranski–Krastanow QDs.[14-17]

Among all the III−V compound semiconductors, GaAsP is one of the most promising choices for photovoltaics, because its band gap can cover wavelengths ranging from green (550 nm) to near infrared (860 nm) at room temperature. It has been predicted that a two-junction tandem solar cell(SC), consisting of a 1.7 eV GaAsP NW junction and a 1.1 eV Si junction, has a theoretical efficiency of 33.8% at 1 sun AM1.5G and 42.3% under 500 suns AM1.5D concentration.[18] If this 1.7/1.1 eV two-junction device is used in water splitting, it is potential to achieve an efficiency of 27.0%.[19]

Despite all these advantages, the development of GaAsP NWs remains stagnant, due to the great challenges in controlling P and the difference in the properties of As and P. For quite a long time, GaAsP research was carried out via vapour-liquid-solid (VLS) growth mode with the help of Au catalyst that could cause serious contamination and hence degrade the performance of devices. In this work, we developed the self-catalyzed GaAsP NW growth technique and achieved high-quality core-shell NWs on both un-patterned and patterned Si substrates. The application of those NWs were demonstrated by making single NW solar cells and large-area water splitting cells.

2. EXPERIMENT

The GaAsP NWs were grown on 380-μm-thick p-doped silicon (111) substrates by a solid-source molecular beam epitaxy. The core NWs were grown by Ga-catalyzed vapor-liquid-solid (VLS) growth mode.[20] If not specially noted, for the growth on un-patterned substrates, the beam equivalent pressures of Ga, III/V ratio, P percentage in GaAsP NWs in

*Huiyun.liu@ucl.ac.uk

Quantum Sensing and Nano Electronics and Photonics XIV, edited by Manijeh Razeghi,
Proc. of SPIE Vol. 10111, 101110X · © 2017 SPIE · CCC code: 0277-786X/17/$18
doi: 10.1117/12.2250588

the flux were 8.72×10^{-8} Torr, 40~50 and 12%, respectively. The substrate temperature was kept at ~640°C as measured by a pyrometer for the growth of core GaAsP nanowires. After the growth of the nanowire cores, the Ga droplets were crystallized into GaAsP by closing the Ga shutter and keeping As and P fluxes. Subsequently, the shell growth was carried out by reopening the Ga flux at the substrate temperatures ~500°C for 1 hour with As and P fluxes at 2.83×10^{-6} and 1.53×10^{-6} Torr, respectively. The patterned growth was on Si(111) substrates with the SiO_2 patterned prepared using nanoimprint lithography. The NWs were grown at a temperature ~630 °C for 45 min with a Ga flux of 1.6 × 10−7 Torr, V/III flux ratios between 3 and 20, and a P/(P + As) flux ratio of 12%. Further details can be found elsewhere.[21-23] The NW morphology was measured by a Zeiss XB 1540 focus ion beam/scanning electron microscopes (FIB/SEM) system. The transmission electron microscope (TEM) analysis was performed on JEOL 2100 and JEOL ARM200F microscopes operating at 200 kV. Compositional analysis using energy-dispersive X-ray spectrometry (EDX) was performed using Oxford Instruments 40 mm^2 SDD EDX detectors.

3. RESULTS AND DISCUSSION

Fig.1 shows the NW tile view and side view of the core-only NWs grown on unpatterned Si substrates. As can be seen, GaAsP NWs are highly uniform in length and diameter. As confirmed in Fig.1c, the length and diameter histogram over 400 NWs show the narrow distribution. The average NW length ($\bar{X}$), root-mean-square deviation (RMSD) and uniformity index (UI) are used to describe the NW length information and are defined by the following equations:

$$\bar{X} = \frac{1}{n}\sum_{i=1}^{n} X_i \quad (1)$$

$$\mathrm{RMSD} = \sqrt{\frac{1}{n}\sum_{i=1}^{n} (X_i - \bar{X})^2} \quad (2)$$

$$\mathrm{UI} = 100\% * (\bar{X} - \mathrm{RMSD})/\bar{X} \quad (3)$$

where the n is the number of NWs that were used in the summation. According to the calculation, this sample has an $\bar{X}$, RMSD and UI of 3.879um, 256nm and 93.4%, respectively. This good NW length uniformity is highly favorable for NW device fabrication.

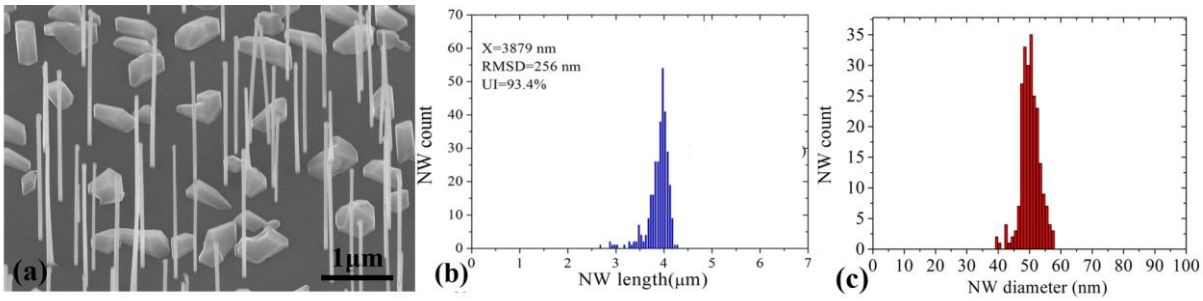

Figure 1. (a) 35° tilted view and (b) length and diameter summation histogram (c) diameter summation histogram of GaAsP NWs.

The incorporation feature of the P was investigated by comparing it with that of the As. The P/(P+As) in the NW as a function of that in the flux was shown in Figure 2a. As can be seen, by adjusting the P/As flux ratio, the GaAsP NWs with a P content ranging from 10% to 75% can be achieved. Moreover, the incorporation coefficient of P was found to be about three times as big as that of the As. This is in stark contrast to the thin film planar epitaxial growth by gas-source or solid-source MBE,[24,25] in which the As has much higher incorporation coefficient compared with that of P. This is because that the incorporation ratio of P/As in the thin film growth is governed by the physical properties; while that of the NW growth is controlled by the chemical properties. As illustrated in Figure 2b, in the VS epitaxial growth mode, the growth is under group V rich conditions and the growth rate is controlled by group III, such as Ga. If the group V adatoms are unable to meet the group III adatoms, they cannot incorporate into the lattice and will desorb from the substrate surface back into the vapor. As adatoms have a larger sticking coefficient and hence longer surface lifetime and migration length than those of P adatoms, which increase the As adatoms' chance of meeting Ga adatoms and incorporating into the lattice. Thus, As incorporation coefficient is higher. By contrast, NWs are grown via the VLS growth mode, which is under a group III rich environment (Figure 2c). The growth is group V element limited, and the

incorporation ratio of P/As is nucleation determined. P has much stronger chemical potential, which endows it higher incorporation efficiency.

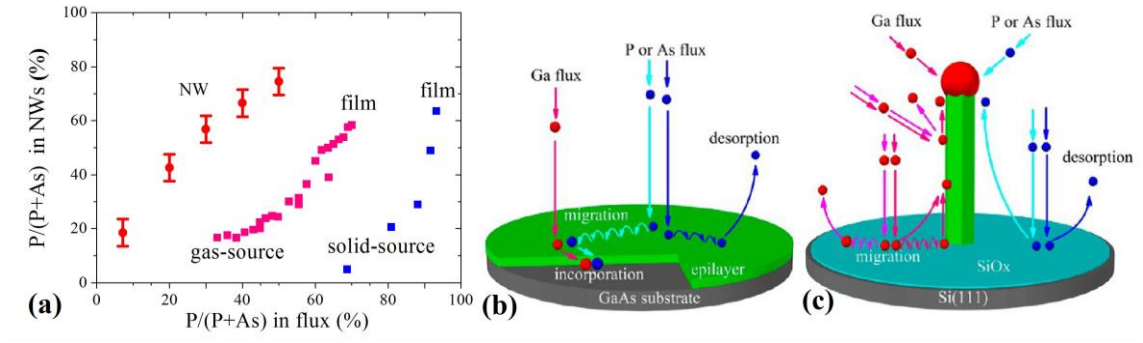

Figure 2. (a) P content as a function of P/(P + As) beam flux ratio during GaAsP growth. Red dots are P content in NWs as a function of P/(P + As) beam flux ratio. The blue and pink dots show the planar GaAsP film growth by solid-source[24] and gas-source MBE,[25] respectively. Schematic illustration of the MBE growth model for (b) the thin film via vapor−solid epitaxial growth mode and (c) the NW via vapor−liquid−solid mode.

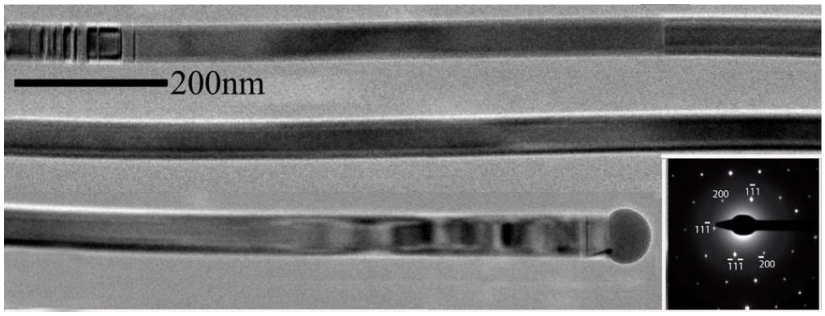

Figure. 3. TEM images of a GaAsP NW. the inset is the electron diffraction pattern

The crystal quality of the NWs was checked by TEM measurement. As can be seen in Figure 3, those NWs are uniform in diameter along the NW length. At the tip of the NW, there is a droplet, which shows that those NWs were grown by Ga-catalyzed VLS mode. For the VLS growth mode, the droplet size decides the NW diameter if there is no VS lateral sidewall growth. Therefore, the homogeneous diameter along the NW length reflects that the Ga droplet size was constant during the growth. This further reveals the well-balanced replenishment and consumption of the Ga in the droplets under this V/III ratio. The body of the NW is almost defect-free with only some occasional twin planes. Those NWs have a ZB crystal structure, as confirmed by the electron diffraction pattern shown in the insets. Defects are present at the very tip and very bottom parts. The bottom defects could be due to the slight fluctuation of growth environment at the initial stage. The defects at the tip should be due to the change of growth parameters during the termination of the NW growth.

With these high-quality GaAsP core NWs, GaAs QDs was inserted (Fig. 4a and b). By carefully control the chemical potential of the droplet, pure-ZB GaAs dots with abrupt interfaces have been achieved (Fig. 4c). Without any surface protection layer, an exciton emission line width as narrow as 130 μeV has been observed (Fig. 4d), which demonstrated great potential in the field of quantum information and nano-photonics.

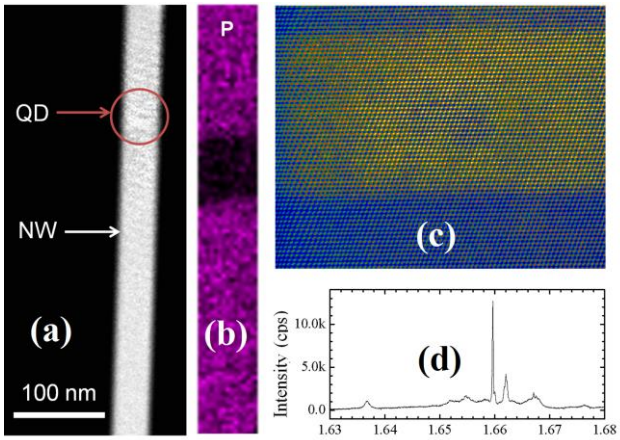

Figure 4. (a) Low-magnification TEM image of a GaAs QD imbedded in a GaAsP nanowire. (b) EDX mapping of the QD region of the nanowire, which shows a higher content of As and negligible content of P compared with the rest of the nanowire. (c) False-colored high-magnification angular dark-field image and (d) the μ-PL spectra of a GaAs QD.

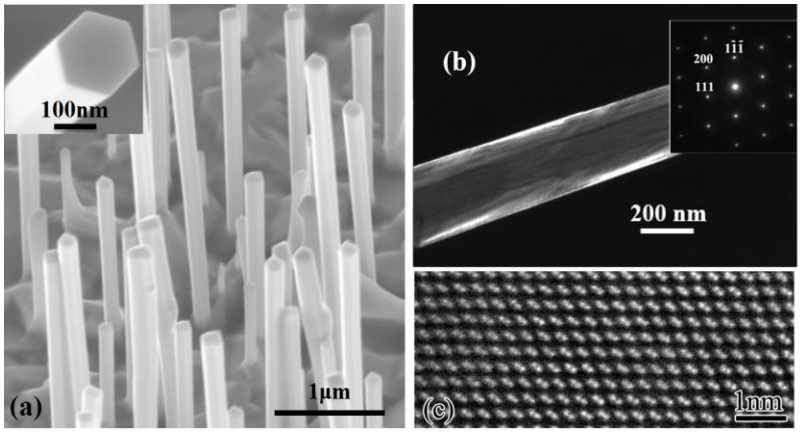

Figure 5. (a) 25° tilted SEM image, (b) Conventional ADF-TEM image and (c) High-magnification annular dark field image of core-shell GaAsP NWs. The inset in (a) is zoom in SEM image of a NW tip and the inset in (b) is electron diffraction pattern.

On the core NW, a layer of shell with the same composition was grown. As can be seen in Figure 5a, the NWs have very smooth on side facets and highly regular tip. The same as the core NW, the defects are mainly concentrated at the very tip and bottom part, leaving the body part almost defect free. As confirmed by the TEM measurement shown in Figure 5b and c, the segment presented is completely defect-free. The shell has the zinc blend crystal structure which is copied from the core NW.

In the cross section of the core-shell GaAsP NWs shown in Figure 6a, we observed the compositional phase segregation, shown as P-rich bands along the six <112> directions in the cross-section. They initiate at the outer corners of the core and extend radially to reach the outer vertices of the shell (Figure 6b). This phenomenon can be explained by the curvature-induced high surface chemical potential at the small {112} facets, which drives away the longer diffusion length element (As) more efficiently (Figure 6c). Moreover, the six P-rich bands can be divided into two groups with different P content. Due to the alternating arrangement of the two types of bands about the NW axis, they are found to have a quasi-3-fold symmetry. The three bands with higher P content are along <112>A directions and those with a lower P content are along <112>B. This polarity-driven symmetry is proposed to be due to the stronger (weaker) bonding energy of {112}B ({112}A) facets with the group-V adatoms, which can reduce (increase) the diffusion length difference between As and P (Figure 6d). These results can help understanding the underlining mechanism of the compositional phase segregation in the multicomponent shell growth, which is beneficial for the growth condition optimization. Moreover, it can also provide valuable information in developing novel NW structure by using the compositional phase segregation, such as growing nanosheets into the NW.

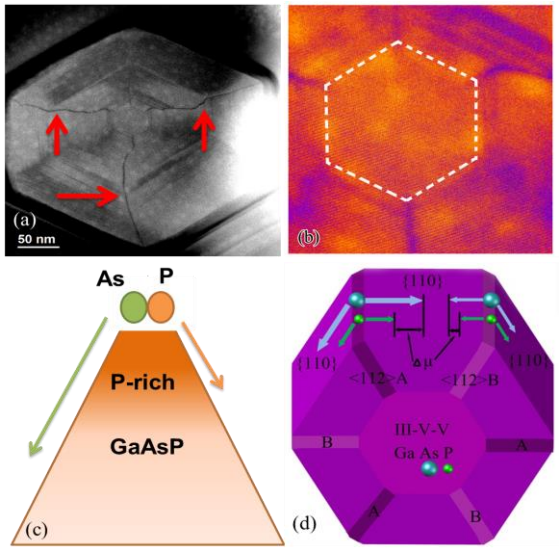

Figure 6. (a) ADF-STEM image of the GaAsP core-shell NW cross-section. (b) ADF-STEM image at the centre of the NW cross-section. (c) and (d) Illustrations of the phase segregation mechanism happened in the shell made of III-V-V materials.

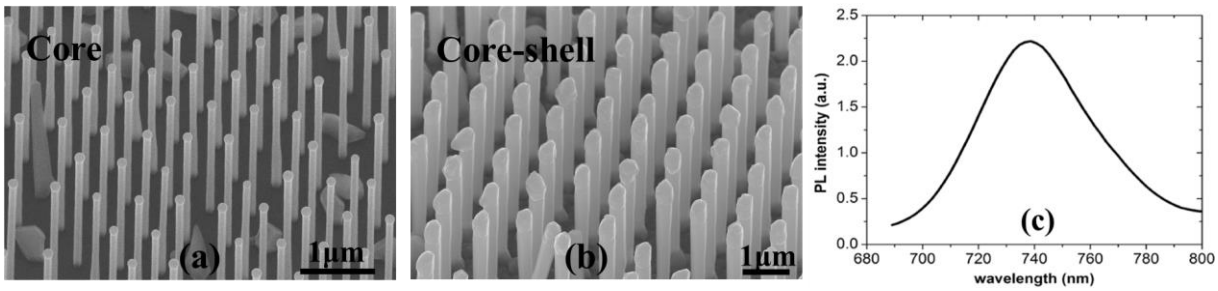

Figure 7. SEM image of the (a) core and (b) core-shell GaAsP NW arrays (tilt angle = 25°), (c) room-temperature photoluminescence of the core-shell GaAsP NW arrays.

To achieve better position control of the NWs, patterned Si substrates were used. However, the growth on patterned Si substrates are challenging. We found that the oxide inside the patterned holes is the key factor that causing the long-term low-repeatability issue. Even with HF solution clean, the hole is still not clean enough. To remove the oxide inside the holes, an in-situ thermal cleaning is needed prior to the NW growth by heating the substrates up to ~900 ^{o}C for 20 minutes. With this step, holes can be fully open by the effective oxide removal. However, the too large oxide-free area inside the holes can cause fast Ga nucleation and hence hinder the formation of Ga droplets. To initiate the NW growth after the hole cleaning, a Ga pre-deposition step was demonstrated to be critical to form Ga droplet. As can be seen in Figure 7a, with the hole cleaning step and Ga pre-deposition technique, the VLS growth of NWs with uniform morphology has been achieved. The core-shell GaAsP NWs on patterned Si substrates (Figure 7b) have good room-temperature emission with peak intensity at ~740 nm, which exhibits their good crystal quality and demonstrates their potential application in photovoltaics, visible emitters, and photonic crystals. These results open up new perspectives for integrating position-controlled III−V NW photonic and electronic structures on a Si platform.

Single-NW Solar cells (SNSCs) were made by fabricating p–i–n core-shell GaAsP nanowires. The surface of the SNSC was covered by a shell of ~10nm highly n-doped InGaP to passivate the surface states. The SNSCs were characterized individually by measuring current-voltage curves in the dark and under AM1.5G illumination. The key parameters of the performance are show in Fig.8 and table 1. A new world record efficiency of 10.2% [2] has been achieved for single NW solar cells, which demonstrates the feasibility of making high-efficiency GaAsP NW solar cells.

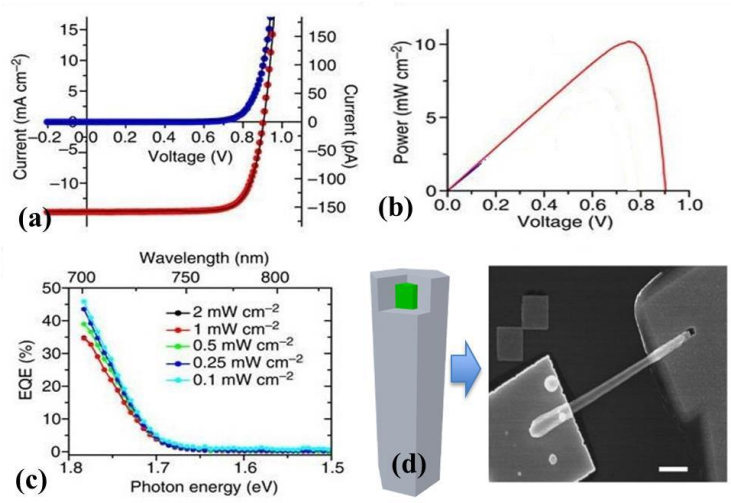

Figure. 8 (a) I-V characteristics under dark (blue dots) and AM1.5G illuminated conditions (red dots), (b) P–V Characterization, (c) External quantum efficiency (EQE) versus photon energy (d) A scanning electron microscope image of the single NW solar cell

Table I. Key performance parameters of single NW solar cells

Efficiency (%)	I_{sc} (mA cm^{-2})	V_{oc} (V)	FF	Ideality factor
10.2	14.7	0.9	0.77	2.0

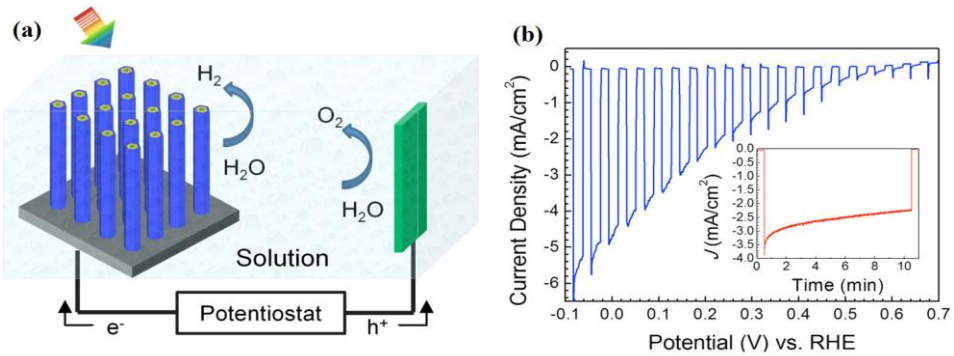

Figure 9. (a) PEC water splitting device structure for GaAsP nanowires grown on Si substrates. (b) Current density potential characteristics of GaAsP homojunction nanowires photocathode.

The application of the GaAsP NWs in the water splitting has also been investigated and results are shown in Figure 9. A wafer-scale solar-to-hydrogen conversion efficiency of 0.5% has been achieved for the GaAsP NW photocathode with a low surface coverage of ~1.8×10^8 cm^{-2}. This STH conversion efficiency is higher than the values previously published for III−V nanowire photoelectrodes fabricated through self-catalyzed approach on a large-scale and could be significantly increased by further improving the density and material quality of GaAsP nanowires. This study paves the way for the development of low-cost and high-efficiency 1.7 eV/1.1 eV GaAsP/silicon tandem PEC cells.

4. CONCLUSION

The growth of self-catalyzed high-quality core-shell GaAsP NWs have been achieved on both patterned and un-patterned Si substrates. NWs are highly uniform in morphology with almost stacking-fault-free zinc-blend crystal

structure. The ternary III-V-V NW growth mechanism and a special polarity-driven quasi-3-fold composition symmetry phenomenon were also investigated in detail. Their potential application on photovoltaic has been demonstrated by single NW solar cells with a world record efficiency exceeding 10% and water splitting devices with a wafer-scale solar-to-hydrogen conversion efficiency of 0.5%. Those results provide valuable information in NW growth mechanism and show the good perspective for photovoltaic devices.

5. REFERENCES

[1] Zhang, Y., Wu, J., Aagesen, M., Liu, H., "III–V nanowires and nanowire optoelectronic devices," J. Phys. D: Appl. Phys., 48 (46), 463001 (2015).

[2] Lieber, C. M., Wang, Z. L., "Functional nanowires". Mrs Bulletin, 32(02), 99-108(2007).

[3]Yan, R., Gargas, D., & Yang, P., "Nanowire photonics". Nature Photonics, 3(10), 569-576 (2009).

[4] Yang, P., Yan, R., Fardy, M., "Semiconductor nanowire: what's next? " Nano letters, 10(5), 1529-1536 (2010).

[5] Lee, A., Liu, H., Seeds, A., "Semiconductor III–V lasers monolithically grown on Si substrates". Semiconductor Science and Technology, 28(1), 015027(2013).

[6] Lee, A., Jiang, Q., Tang, M., Seeds, A., Liu, H., "Continuous-wave InAs/GaAs quantum-dot laser diodes monolithically grown on Si substrate with low threshold current densities". Optics express, 20(20), 22181-22187(2012).

[7] Tang, M., Chen, S., Wu, J., Jiang, Q., Dorogan, V. G., Benamara, M., Mazur, Y. I., Salamo, G J., Seeds, A., Liu, H., "1.3-μm InAs/GaAs quantum-dot lasers monolithically grown on Si substrates using InAlAs/GaAs dislocation filter layers". Opt. Express, 22(10), 11528-11535 (2014).

[8] Wu, J., Lee, A., Jiang, Q., Tang, M., Seeds, A. J., Liu, H., "Electrically pumped continuous-wave 1.3-μm InAs/GaAs quantum dot lasers monolithically grown on Si substrates". IET Optoelectronics, 8(2), 20-24 (2014).

[9] Mohseni, P. K., Behnam, A., Wood, J. D., English, C. D., Lyding, J. W., Pop, E., & Li, X., "In x Ga1–x As Nanowire Growth on Graphene: van der Waals Epitaxy Induced Phase Segregation". Nano letters, 13(3), 1153-1161 (2013).

[10] Munshi, A. M., Dheeraj, D. L., Fauske, V. T., Kim, D. C., van Helvoort, A. T., Fimland, B. O., Weman, H., "Vertically aligned GaAs nanowires on graphite and few-layer graphene: generic model and epitaxial growth". Nano letters, 12(9), 4570-4576(2012).

[11] Ikejiri, K., Ishizaka, F., Tomioka, K., Fukui, T., "GaAs nanowire growth on polycrystalline silicon thin films using selective-area MOVPE". Nanotechnology, 24(11), 115304(2013).

[12] Holm, J. V., Jørgensen, H. I., Krogstrup, P., Nygård, J., Liu, H., Aagesen, M., "Surface-passivated GaAsP single-nanowire solar cells exceeding 10% efficiency grown on silicon". Nature communications, 4, 1498 (2013).

[13] Wu, J., Ramsay, A., Sanchez, A. M., Zhang, Y., Kim, D., Brossard, F. S. F., Salamo, G. G. (2015). "Defect-free self-catalyzed GaAs/GaAsP nanowire quantum dots grown on silicon substrate". Nano Letters. Nano letters, 16(1), 504-511(2016).

[14] Liu, H. Y., Steer, M. J., Badcock, T. J., Mowbray, D. J., Skolnick, M. S., Suárez, F., Ng, J. S., Hopkinson, M., David, J. P. R. (2006). "Room-temperature 1.6 μm light emission from InAs/GaAs quantum dots with a thin GaAsSb cap layer". Journal of applied physics, 99, 046104.

[15] Liu, H. Y., Sellers, I. R., Badcock, T. J., Mowbray, D. J., Skolnick, M. S., Groom, K. M., Gutierrez, M., Hopkinson, M., Ng, J. S., David, J. P. R., Beanland, R., "Improved performance of 1.3 mum multilayer InAs quantum-dot lasers using a high-growth-temperature GaAs spacer layer". Applied Physics Letters, 85, 704 (2004).

[16] Liu, H. Y., Hopkinson, M., Harrison, C. N., Steer, M. J., Frith, R., Sellers, I. R., Mowbray, D. J., Skolnick, M. S., "Optimizing the growth of 1.3 μm InAs/InGaAs dots-in-a-well structure". Journal of applied physics, 93(5), 2931-2936 (2003).

[17] Liu, H. Y., Sellers, I. R., Gutierrez, M., Groom, K. M., Soong, W. M., Hopkinson, M., David, J. P. R., Beanland, R., Badcock, T. J., Mowbray, D. J., Skolnick, M. S., "Influences of the spacer layer growth temperature on multilayer InAs/GaAs quantum dot structures". Journal of applied physics, 96, 1988-1992 (2004).

[18] LaPierre, R. R., "Theoretical conversion efficiency of a two-junction III-V nanowire on Si solar cell". Journal of Applied Physics, 110(1), 014310 (2011).

[19] Walter, M. G., Warren, E. L., McKone, J. R., Boettcher, S. W., Mi, Q., Santori, E. A., Lewis, N. S., "Solar water splitting cells". Chemical reviews, 110(11), 6446-6473 (2010).

[20] Zhang, Y., Wu, J., Aagesen, M., Holm, J., Hatch, S., Tang, M., Huo, S., Liu, H. (2014). "Self-Catalyzed Ternary Core–Shell GaAsP Nanowire Arrays Grown on Patterned Si Substrates by Molecular Beam Epitaxy". Nano letters, 14(8), 4542-4547.
[21] Zhang, Y., Aagesen, M., Holm, J. V., Jørgensen, H. I., Wu, J., Liu, H., "Self-catalyzed GaAsP nanowires grown on silicon substrates by solid-source molecular beam epitaxy". Nano letters, 13(8), 3897-3902 (2013).
[22] Zhang, Y., Sanchez, A. M., Wu, J., Aagesen, M., Holm, J. V., Beanland, R., Ward, T., Liu, H., Polarity-"Driven Quasi-3-Fold Composition Symmetry of Self-Catalyzed III–V–V Ternary Core–Shell Nanowires". Nano letters, 15(5), 3128-3133 (2015).
[23] Wu, J., Li, Y., Kubota, J., Domen, K., Aagesen, M., Ward, T., Sanchez, A., Beanland, R., Zhang, Y., Tang, M., Hatch, S., Seeds, A., "Wafer-scale fabrication of self-catalyzed 1.7 eV GaAsP core–shell nanowire photocathode on silicon substrates". Nano letters, 14(4), 2013-2018 (2014).
[24] Shu-Dong, W., Li-Wei, G., Wen-Xin, W., Zhi-Hua, L., Ping-Juan, N., Qi, H., & Jun-Ming, Z., "Incorporation Behaviour of Arsenic and Phosphorus in GaAsP/GaAs Grown by Solid Source Molecular Beam Epitaxy with a GaP Decomposition Source". Chinese Physics Letters, 22(4), 960 (2005).
[25] Hou, H. Q., Liang, B. W., Chin, T. P., Tu, C. W., "Insitu determination of phosphorus composition in GaAs1− xPx grown by gas‐source molecular beam epitaxy". Applied physics letters, 59(3), 292-294 (1991).